Resveratrol Stimulates Mitochondrial Bioenergetics to Protect Retinal Pigment Epithelial Cells From Oxidative Damage

Shwu-Jiuan Sheu,[1,2] Ni-Chun Liu,[1,3] Chen-Chun Ou,[4] Youn-Shen Bee,[1] Shih-Chou Chen,[1] Hsiu-Chen Lin,[1] and Julie Y. H. Chan[4]

[1]Department of Ophthalmology, Kaohsiung Veterans General Hospital, Kaohsiung, Taiwan
[2]School of Medicine, National Yang-Ming University, Taipei, Taiwan
[3]Institute of Biological Science, National Sun Yat-sen University, Kaohsiung, Taiwan
[4]Center for Translational Research in Biomedical Science, Kaohsiung Chang Gung Memorial Hospital, Kaohsiung, Taiwan

Correspondence: Julie Y. H. Chan, Center for Translational Research in Biomedical Science, Kaohsiung Chang Gung Memorial Hospital, Kaohsiung, Taiwan; jchan@adm.cgmh.org.tw.

Submitted: March 13, 2013
Accepted: August 21, 2013

Citation: Sheu S-J, Liu N-C, Ou C-C, et al. Resveratrol stimulates mitochondrial bioenergetics to protect retinal pigment epithelial cells from oxidative damage. *Invest Ophthalmol Vis Sci.* 2013;54:6426–6438. DOI:10.1167/iovs.13-12024

Purpose. Resveratrol (RSV) alleviates oxidative damage in human adult retinal pigment epithelial (ARPE) cells. Mitochondrial bioenergetics is associated with oxidative stress. The purpose of this study was to examine the role of mitochondrial bioenergetics in the cytoprotective effect of RSV. Its role in protection against the adverse effects of cigarette smoke (CS) in experimental choroidal neovascularization (CNV) was also examined.

Methods. Cultured ARPE-19 cells were treated with acrolein alone or acrolein with added RSV. Temporal changes in cell viability, expression of the antioxidant protein, and mitochondrial bioenergetics were evaluated. In an animal study, CNV lesions were created in Brown Norway rats by laser-induced photocoagulation. Effects of CS alone or with additional RSV treatment on CNV lesions were quantified by fundus fluorescein angiography.

Results. In ARPE-19 cells, RSV rescued acrolein-induced cell death, alongside reversal of acrolein-induced superoxide dismutase expression. Resveratrol increased the mitochondrial bioenergetics, including basal respiratory rate, adenosine triphosphate synthesis via oxidative phosphorylation, and maximal mitochondrial capacity. In animal experiments, CS induced a significant increase in CNV following laser injury, and this increase in CNV was appreciably prevented following peripheral infusion of RSV.

Conclusions. Our results indicate that RSV, a major polyphenol found in red wine, exerts protection against acrolein-induced cytotoxicity in human ARPE-19 cells via increases in the mitochondrial bioenergetics. In addition, the antioxidant effect of RSV may contribute to protection against laser-induced CNV in animals exposed to CS. Therefore, RSV might be beneficial for treatment of acrolein-induced or CS-evoked RPE degeneration.

Keywords: mitochondrial bioenergetics, retinal pigment epithelium, resveratrol, choroidal neovascularization, superoxide dismutase

Age-related macular degeneration (AMD) is one of the major causes of adult visual loss. Loss of vision in AMD patients results from photoreceptor death in the central retina, but the early pathogenesis involves apoptosis of retinal pigment epithelial (RPE) cells.[1,2] Emerging evidence suggests an important role of oxidative stress in the development of RPE apoptosis.[3–5] Eyes obtained postmortem from AMD patients display extensive free radical damage to RPE cells.[6] Oxidative stress induced by chemical oxidants induces RPE cell death.[7–10] Conversely, protection against oxidative stress by adequate intake of dietary antioxidants delays or prevents apoptosis of RPE cells and the development of retinal diseases.[11–13]

The mitochondria are well-defined cellular sources for generation of the reactive oxygen species (ROS). Retinal pigment epithelium is subjected to high oxygen tension due to its juxtaposition to the blood supply of the choriocapillaris, which exhibits high flow rate and oxygen saturation levels. As such, RPE cells are enriched with mitochondria for a robust metabolic activity to meet the high-energy demands of the cells.[14] During the process of oxidative phosphorylation for production of adenosine triphosphate (ATP), high concentrations of ROS are generated locally in mitochondria of the RPE cells. When the mitochondrial-derived ROS exceed the cellular antioxidant defense capacity, as a consequence of aging, ROS accumulate in the mitochondria, inducing damage to the RPE cells.[15–17]

Smoking is a significant risk factor associated with the prevalence and incidence of neovascularization in AMD.[18,19] The linkage between smoking and AMD has been supported by several large epidemiological studies, including the Age-Related Eye Disease Study.[20–22] Smoking is a cause of severe oxidative stress due to the high concentrations of aldehydes and nitrites in cigarette smoke.[23–25] It is now recognized that major toxicants in cigarette smoke, including acrolein, acetaldehyde, acrylonitrile, benzene, 1,3-butadiene, and formaldehyde, are of particular concern regarding health risk.[26] Among these, acrolein is the major cause of the onset and progress of

AMD[27,28] via induction of oxidative damage in RPE cells, although the underlying mechanism is not fully understood.

Resveratrol (RSV), a major active ingredient of stilbene phytoalexins that was first isolated from the roots of the oriental medicinal plant *Polygonum capsidatum,* is a plant antibiotic that exhibits a strong antifungal property.[29] In addition, RSV exhibits antioxidant activity.[30–32] In animal studies, RSV has been shown to prevent ocular inflammation in endotoxin-induced uveitis[31] and glaucoma.[33] In view of a potent cytoprotective effect of RSV, cellular responses induced by RSV warrant further investigation.

We reported previously that RSV alleviates oxidative impairment of the phagocytotic function in human RPE cells.[34] Similar protection was observed in the ultraviolet irradiation damage model of human RPE cells.[35] The purpose of this study was to examine the roles of mitochondrial bioenergetics and redox status in the cytotoxic effect of acrolein and their involvement in RSV-induced cell protection. The protective effect of RSV against experimental choroidal neovascularization (CNV) was also examined.

Methods

Chemicals

Acrolein, resveratrol (purity≧, 98%), and coenzyme Q_{10} (CoQ_{10}; purity≧, 98%) were purchased from Sigma-Aldrich Chemical Co. (St. Louis, MO). Reagents and materials for cell culture were obtained from GIBCO (Life Technologies, Inc., Grand Island, NY).

Cell Culture

Adult human retinal pigment epithelial cells (ARPE-19) were obtained from American Type Culture Collection (ATCC No. CRL-2302; Manassas, VA). These cells were maintained in a 1:1 mixture of Dulbecco's modified Eagle's medium (DMEM) and Ham's F12 medium supplemented with 10% fetal bovine serum (Life Technologies, Inc.), sodium bicarbonate (1.2 g/L), L-glutamine (2.5 mM), HEPES (15 mM), and sodium pyruvate (0.5 mM). The cells were cultured at 37°C in a humidified atmosphere of 95% air and 5% CO_2.

For primary culture of RPE cells, the cells were isolated from eye tissues of adult female Brown Norway pigmented rats subjected to experimental treatments, according to previously reported procedures.[36] In brief, after the vitreous and the neural retina were removed, the eye cups were washed and incubated in Eagle's minimum essential medium (Life Technologies, Inc.) with 0.05% trypsin (Fisher Scientific, Ottawa, ON) and 0.02% EDTA (Fisher Scientific) for 1 hour. This was followed by the release of RPE cells by gentle pipetting. The collected cells were washed twice and plated in flasks in Ham's F12 medium (Life Technologies, Inc.) supplemented with 10% fetal bovine serum. The RPE cells were incubated at 37°C in a humidified incubator of 5% CO_2 and 95% air. The media were changed every 2 days to provide sufficient nutrition. Epithelial cells were identified by their characteristic cobblestone appearance in confluent cell culture. Cultured cells between passages 4 and 10 were used for this study.

Animals

Adult female Brown Norway pigmented rats (body weight: 200–265 g) purchased from the Experimental Animal Center of the National Applied Research Laboratories, Taiwan, were used. All experimental procedures were carried out in compliance with the guidelines of our Institutional Animal Care and Use Committee. The animals were handled in accordance with the ARVO Statement for the Use of Animals in Ophthalmic and Vision Research. The rats were anesthetized by intramuscular injection of an equal-volume mixture of 2% lidocaine (0.15 mL/kg; Astra Södertälje, Karlebyhus, Sweden) and ketamine (50 mg/mL; Parke-Davis, Morris Plains, NJ). All surgical procedures were performed using sterilized instruments. Animals were allowed to acclimatize for at least 7 days before experimental manipulations.

Cell Viability Assay

The viability of cells was tested by 3-(4,5-cimethylthiazol-2-yl)-2,5-diphenyl tetrazolium bromide (MTT) and lactate dehydrogenase (LDH) assays according to the protocols described previously.[34,37] For MTT assay, the ARPE-19 cells were seeded at 3×10^3 per well in a 96-well plate. The cells were stimulated with acrolein (25 μM) alone or acrolein with added RSV (10 or 20 μM) or CoQ_{10} (50 μM) for 24, 48, or 72 hours. Dose of acrolein was adopted from studies that used this toxin in ARPE-19 cells for the same purpose.[38] Concentrations of RSV and CoQ_{10} were adopted from previous studies[34,39] or selected based on our pilot studies in which these agents exhibited protection against acrolein-induced cell damage. At the end of each treatment, the cells were washed with medium, followed by addition of MTT (0.5 mg/mL) to the medium for quantification of metabolically active living cells. The plate was incubated at 37°C for 4 hours. The dark-blue formazan crystals formed by living cells were dissolved in 150 μL dimethyl sulfoxide (DMSO), and absorbance for individual wells at 555 nm was measured with a microplate spectrophotometer (Spectra Max 340; Molecular Devices, Sunnyvale, CA). Absorbance values were normalized with those of untreated cells to calculate the changes in cell viability. In some experiments, cell membrane integrity was determined using LDH assay.[37] After the various treatments, supernatants were collected, and LDH release was quantified for 1 minute at 340 nm in a reactive mixture containing culture medium, sodium pyruvate (0.18 mM), and nicotinamide adenine dinucleotide (NADH, 0.60 mM). The LDH released into the media was analyzed to determine LDH activity using an analysis kit according to the manufacturer's instructions (Biochain Institute, Hayward, CA). Lactate dehydrogenase activity in each cell lysate was expressed as the percentage of control (100%).

Western Blot Analysis

Cells were rinsed twice with cold PBS, and total protein was extracted with ice-cold lysis buffer (Cell Signaling Technology, Beverly, MA) supplemented with protease inhibitor cocktail (Roche Diagnostics Ltd., Mannheim, Germany), sodium fluoride (10 mM), and phenylmethylsulphonyl fluoride (1 mM) to prevent protein degradation. Cells were scraped and forced through a thin needle two or three times. The lysates were incubated for 20 minutes on ice and centrifuged at 15,000*g* at 4°C for 20 minutes. Supernatants were transferred into fresh tubes. Protein concentration was measured using a modified Lowry protein assay kit (Thermo Scientific, Rockford, IL).

Equal aliquots (10 μg) of protein were separated using 12% SDS-PAGE and transferred to polyvinylidene fluoride membrane for 1.5 hours at 4°C, using a Bio-Rad (Hercules, CA) miniprotein-III wet transfer unit. The transfer membranes were then incubated with blocking solution (5% nonfat dried milk dissolved in Tris-buffered saline–Tween buffer [pH 7.6], 10 mM Tris-HCl, 150 mM NaCl, and 0.1% Tween 20) for 1 hour at room temperature. The membranes were incubated with a rabbit polyclonal antibody against copper/zinc superoxide dismutase (Cu/ZnSOD, 1:2000), manganese SOD (MnSOD, 1:2000), extracellular SOD (ecSOD, 1:2000) (Stressgen Biotechnologies,

Victoria, BC), or α-tubulin (1:10,000; Sigma-Aldrich) at 4°C overnight. This was followed by incubation of the membranes with horseradish peroxidase–conjugated anti-rabbit IgG (1:2000; Jackson ImmunoResearch Laboratories, West Grove, PA) at room temperature for 2 hours. Specific antibody–antigen complex was detected using an enhanced chemiluminescence Western blot detection system (GE Healthcare Bio-Sciences Corp., Piscataway, NJ). The amount of detected protein was quantified by Photo-Print Plus software (ETS Vilber-Lourmat, Marne-la-Vallée, France).

Mitochondrial Respiration and Steady-State ATP Level Measurements

Mitochondrial respiration was assessed using a Seahorse XF24 Extracellular Flux Analyzer (Seahorse Bioscience, North Billerica, MA). ARPE-19 cells were cultured on Seahorse XF-24 plates at a density of 3×10^3 cells/well. The cells were pretreated with RSV (10 or 20 μM) for 48 hours alone or with added acrolein (25 μM) for 24 hours. The sensor cartridge was hydrated with calibration buffer 1 day prior to each experiment. Each well was washed with DMEM solution supplemented with 25 mM glucose, 2 mM sodium pyruvate, 31 mM NaCl, 2 mM GlutaMax (Life Technologies, Inc.), pH 7.4, and incubated at 37°C before the start of the experiment. Baseline measurements of oxygen consumption rate (OCR, measured by oxygen concentration change) and extracellular acidification rate (ECAR, measured by pH change) were taken before sequential injection of treatments/inhibitors: oligomycin (ATP synthase inhibitor), carbonyl cyanide 4-(trifluoromethoxy)phenylhydrazone (FCCP; mitochondrial respiration uncoupler), and antimycin (an electron transport blocker). These agents were injected through ports of the Seahorse Flux Pak cartridges to reach final concentrations of 1, 0.25, and 1 μM, respectively. OCR reading reflects the oxygen consumption rate, whereas the measurement of ECAR reflects lactate production and is used as an index of glycolysis.[40] After basal OCR and ECAR were recorded, oligomycin and FCCP were injected sequentially and changes in OCR and ECAR values were measured. The OCR value measured after oligomycin represents the amount of oxygen consumption linked to ATP production, and that after FCCP injection denotes the maximal mitochondrial respiratory capacity of the cells. The final injection of antimycin inhibits the flux of electrons through complex III, and thus no oxygen is further consumed at complex V. The OCR reading after this treatment is primarily nonmitochondrial and is considered to be due to cytosolic oxidase enzymes.[41] After the assays, plates were saved and protein readings measured for each well to confirm equal cell number per well.

Determination of the Relative Mitochondrial DNA Copy Number

Mitochondrial DNA (mtDNA) was extracted from ARPE-19 cells or primary cultured RPE cells from the animals (approximately 3×10^6 cells) using QIAamp DNA Mini Kit (Qiagen, Hilden, Germany). The DNA pellet was dried by vacuum and then dissolved in distilled water and kept at −20°C until use. Quantitative real-time PCR was used for quantification of DNA.[42] The mtDNA copy number was defined as total mtDNA copies divided by total nuclear DNA (nDNA) copies, after adjusting the mtNDA copy number of control ARPE-19 cells to 100% according to the established standard curves. The sequences of primers used for mtDNA (rat *ND1* region) and nDNA (rat β-actin) amplification were 5′-GAAATCGTGCGTGACATTAAAG-3′ (forward) and 5′-ATCG GAACCGCTCATTG-3′ (reverse) and 5′-ATTCTAGCCACAT CAAGTCTTT-3′ (forward) and 5′-GGAGGACGGATAAGAGGA TAAT-3′ (reverse), respectively. The PCR was performed in a LightCycler 480 System (Roche Applied Science, Mannheim, Germany) using the SYBR Green PCR Master Mix Kit (2X) (Applied Biosystems, Hammonton, NJ).

For each reaction, DNA (10 ng/μL) was mixed with 10 μL SYBR Green PCR Master Mix Kit containing 500 nM forward and reverse primers to a final volume of 20 μL. The PCR conditions were 10 minutes at 95°C followed by 45 cycles of denaturation at 95°C for 10 seconds, annealing at 60°C for 15 seconds, and primer extension at 72°C for 20 seconds. The melting curves analysis was performed using Dissociation Curve Software (Roche Applied Science). The amplified products were denatured and annealed at different temperatures to detect their specific melting temperatures. Samples showing primer-dimers or unspecific fragments were excluded. The threshold cycle number (Ct) values of the β-actin gene and the mitochondrial *ND1* gene were determined for each sample in the same quantitative PCR run. The Ct values were calculated and the relative copy number $(R_c) = 2(2^{\Delta Ct})$, where ΔCt is $Ct_{ND1} - Ct_{\beta\text{-actin}}$. Each reaction was done in duplicate, and experiments were repeated for three independent cell cultures.

Quantitative Reverse Transcription–Polymerase Chain Reaction (qRT-PCR)

Ribonucleic acid was isolated from the ARPE-19 cells using RNAzol (Tel-Test, Inc., Friendswoods, TX). This was followed by further purification in a reaction containing DNase to remove the residual DNA for a better quality of mtDNA that harbors no intron. The purified DNA-free RNA was reverse transcribed to cDNA with the Ready-to-go RT-PCR kit (Invitrogen, Carlsbad, CA). Quantitative real-time PCR was performed in LightCycler 480 System (Roche Applied Science) using a SYBR Green I assay. The PCR reaction was performed in SYBR Green PCR Master Mix kit (2X) (Applied Biosystems) following protocols provided by the manufacturer. The sequences of primers used for human mitochondrial transcription factor A (mtTFA) and human β-actin gene amplification were 5′-CCCATATTTAAAGCTCAGAACCCAGA-3′ (forward) and 5′-TTGAATCAGGAAGTTCCCTCCCA-3′ (reverse) and 5′-GAAATCGTGCGTGACATTAAAG-3′ (forward) and 5′-ATCG GAACCGCTCATTG-3′ (reverse), respectively.

The same PCR conditions used for quantification of mtDNA copies were adopted for measurement of mtTFA gene expression. The threshold Ct values of the mtTFA gene and the β-actin gene were determined for each sample in the same quantitative PCR run. The intraassay coefficients of variation of Ct values were approximately 2.1% and 3.4% for mtTFA and β-actin gene, respectively. Expression of the mtTFA mRNA relative to the β-actin gene was determined by the fold-change analysis $1/2^{\Delta Ct}$, where ΔCt is the $Ct_{mtTFA} - Ct_{\beta\text{-actin}}$. Each reaction was done in duplicate, and experiments were repeated for three independent cell cultures.

Long-Term Exposure of Animals to Cigarette Smoke

For long-term cigarette smoke (CS) exposure, rats were placed in an exposure chamber (20 × 50 × 70 cm) with a narrow orifice connected to a stopcock through which 750 mL fresh CS generated from 1.5 cigarettes (Marlboro Red Label; Philip Morris International, Inc., New York, NY) was delivered.[43] The CS was passed out of the chamber by four exhaust holes (1 cm) on the side panels. During the exposure, the rats were placed in the chamber and allowed to breathe spontaneously for 10 minutes under conscious conditions. After the CS exposure,

the rats were transferred to a new cage and allowed to inspire air. The animals were exposed to CS twice daily at 10 AM and 4 PM for 4 weeks. Control animals underwent identical procedures in the chamber but with exposure to air.

Laser-Induced Choroidal Neovascularization in Rats

The rodent model of laser-induced CNV was adopted from the previously reported procedures with minor modification.[44] In brief, the rats were anesthetized by intramuscular injection of an equal-volume mixture of 2% lidocaine (0.15 mL/kg; Astra Södertälje) and ketamine (50 mg/mL; Parke-Davis), and pupils of both eyes were dilated with 1% tropicamide (Alcon Laboratories, Hünenberg, Switzerland). A piece of cover glass served as a contact lens. Argon laser (Novus Omni; Coherent, Palo Alto, CA) irradiation was delivered through a slit lamp (Carl Zeiss, Oberkochen, Germany). Laser parameters used were as follows: spot size of 50 μm, power of 400 mW, and exposure duration of 0.05 seconds. An attempt was made to break Bruch's membrane, as clinically evidenced by central bubble formation, with or without intraretinal or choroidal hemorrhage. Four lesions were created between the major retinal vessels in each fundus.

Fundus Fluorescein Angiography

Five weeks after laser photocoagulation, sizes of the CNV lesions were studied by fundus fluorescein angiography (FAG) using a digital fundus camera (Visupac 450, Zeiss FF450). Fluorescein sodium (10%, 0.1 mL/kg, Fluorescite; Alcon, Fort Worth, TX) was injected into the intraperitoneal cavity of the anesthetized rats. Late-phase angiograms were obtained 8 minutes after injection, and digital fundus pictures of the eyes were taken within 1 minute. A CNV was defined by the presence of early hyperfluorescence with late leakage at the site of laser injury.[44] In each eye, the areas of CNV on FAG were measured with image analysis software (ImageJ; National Institutes of Health, Bethesda, MD). The mean area of CNV was derived from measurement of all the CNV lesions by an ophthalmologist who was masked to the treatments of the eyes.

Implantation of Osmotic Minipump

On the day of implantation, animals were anesthetized with sodium pentobarbital (50 mg/kg, intraperitoneally), and an osmotic minipump (Alzet 2004; Durect Co., Cupertino, CA) was placed in the peritoneal cavity.[45] Control animals received DMSO-filled osmotic minipumps, and sham-operated animals received identical surgical procedures only. Animals received procaine penicillin (1000 IU, intramuscular) injection postoperatively, and only animals that showed progressive weight gain after the operation were used in subsequent experiments.

Experimental Design for Animal Study

Animals were divided into two groups to receive CS or air exposure for 4 weeks. Before the exposure, each group of animals was subdivided randomly to receive intraperitoneal implantation of an osmotic minipump for continuous infusion of RSV (1.6 mg/kg/d), CoQ_{10} (0.36 mg/kg/d), or vehicle (0.8% DMSO). Concentration of RSV or CoQ_{10} was modified from those used in previous studies[39,46] and determined in our pilot study, which showed effectiveness of the agents to reduce laser-induced CNV. The animals were allowed to recover from surgery for 3 days prior to CS exposure. The laser-induced CNV was performed at the end of 4 weeks of CS or air exposure and quantified 5 weeks after laser irradiation.

Statistical Analysis

Results are presented as means ± SEM. One-way analysis of variance was used to assess group means, followed by the Mann-Whitney *U* test analysis with two-tailed probability. The statistical software SigmaStat (SPSS, Chicago, IL) was used for data analysis. A *P* value less than 0.05 was considered statistically significant.

Results

Protection by Resveratrol Against Acrolein-Induced Decrease in Cell Viability

Acrolein has been implicated in RPE cell death.[34,38,47] We first examined whether RSV protects RPE cells from acrolein-induced cell death. Data from the MTT assay showed that exposure of ARPE-19 cells to acrolein (25 μM) for 24, 48, or 72 hours led to a significant reduction in cell viability (24 hours: 86.9 ± 4.3%; 48 hours: 80.6 ± 4.9%; 72 hours: 72.5 ± 5.6%, $n = 6$) as compared with the control group at each posttreatment time interval (24 hours: 98.6 ± 4.7%; 48 hours: 96.5 ± 3.3%; 72 hours: 96.2 ± 4.8%, $n = 6$) (Fig. 1A). Resveratrol treatment (10 or 20 μM) alone resulted in a dose-related increase in cell viability during the same posttreatment time intervals. The same treatment also appreciably reversed the acrolein-induced decrease in cell viability in ARPE-19 cells. Dimethyl sulfoxide (solvent for RSV), on the other hand, had no discernible effect on the cell viability or acrolein-promoted decrease in cell viability (data not shown). These results demonstrated a protective effect of RSV on survival of ARPE-19 cells with acrolein exposure.

We further performed the LDH assay to consolidate results obtained from the MTT assay. At 24 hours after acrolein (25 μM) exposure, LDH release into the media was significantly increased (Fig. 1B). The acrolein-induced cell toxicity was noticeably prevented in ARPE-19 cells treated with RSV (10 or 20 μM). Similar results were obtained for the ARPE-19 cells exposed to acrolein for 48 or 72 hours (data not shown).

Increases in MnSOD Expression Following Acrolein Exposure

Oxidative stress contributes to acrolein-induced damage to RPE cells.[27,28,34,47] We therefore examined the effect of acrolein on the expression of antioxidant SOD isoforms in ARPE-19 cells. We found that acrolein (1, 10, 25 or 50 μM) exposure for 24 hours caused a dose-dependent increase in protein expression of mitochondrial MnSOD, but not cytosolic Cu/ZnSOD (Fig. 2). Similar responses were observed after exposure of the ARPE-19 cells to acrolein for 48 or 72 hours (data not shown). Expression of extracellular ecSOD in ARPE-19 cells was under our detection limit, and was not affected by acrolein exposure. The observation of an increase in MnSOD expression indicates activation of mitochondrial antioxidant defense mechanism to counterbalance oxidative stress in ARPE-19 cells exposed to acrolein.

Resveratrol Reverses the Increase in MnSOD Expression Induced by Acrolein

To further examine the effect of RSV on acrolein-induced oxidative damage in ARPE-19 cells, RSV (20 μM) was applied to the medium for 48 hours prior to acrolein (25 μM) exposure;

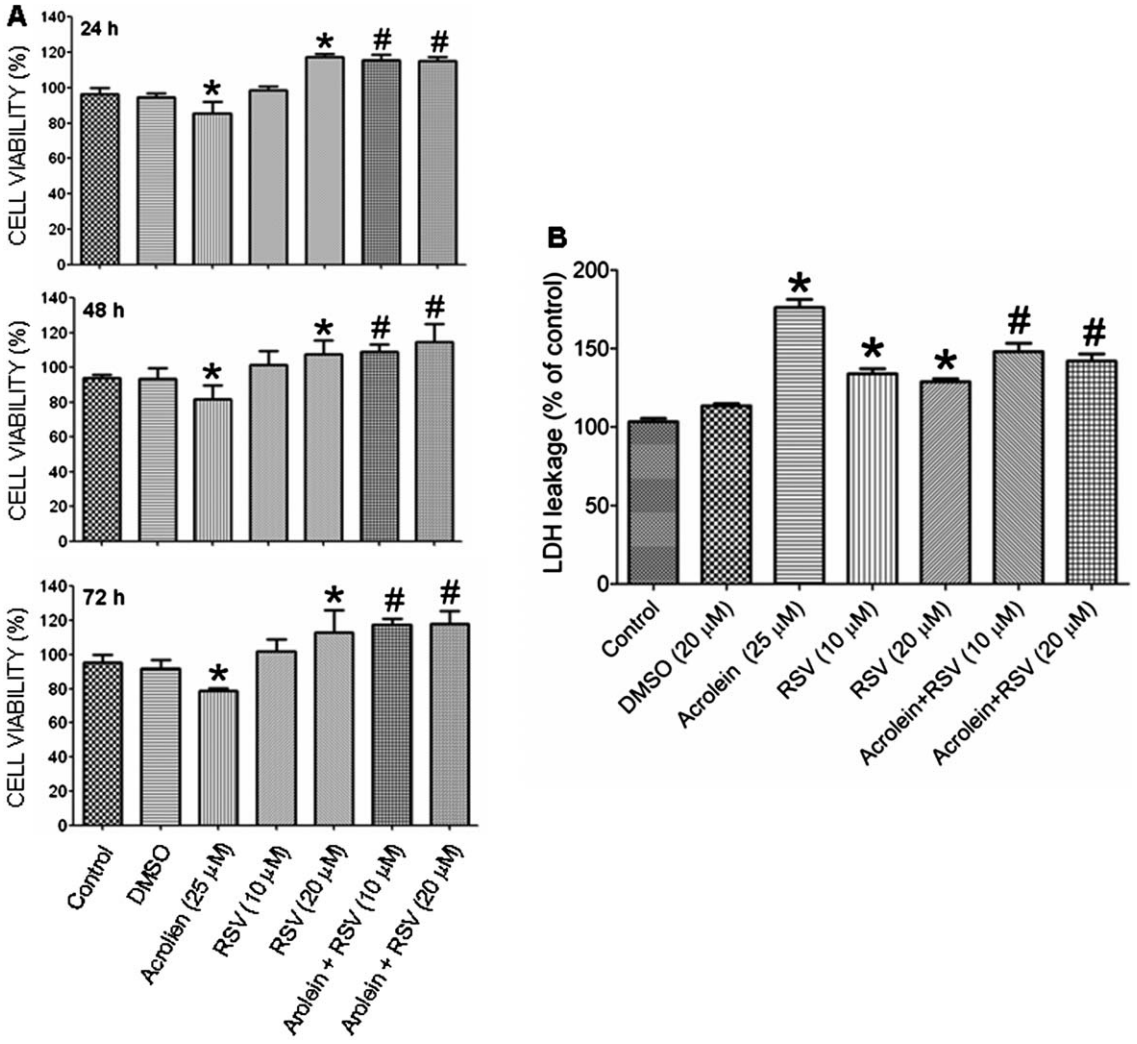

Figure 1. Protection by resveratrol against acrolein-induced decrease in cell viability of ARPE cells. ARPE-19 cells were treated with acrolein (25 μM) alone or with added resveratrol (RSV, 10 or 20 μM) for 24, 48, or 72 hours. Cell viability was assayed with MTT (**A**) or LDH (**B**) assay. Acrolein caused a significant decrease in cell viability, and this induced suppression was prevented by RSV treatment. Analyses were performed in triplicate, and experiments were repeated for three independent cell cultures. Values are mean ± SEM. *$P < 0.05$ versus control group and #$P < 0.05$ versus acrolein-treated cells.

and MnSOD expression in ARPE-19 cells was evaluated 24 hours after acrolein administration. As shown in Figure 3, pretreatment with RSV significantly blunted the increase in MnSOD expression induced by acrolein. A similar response was observed in cells pretreated with a mobile electron carrier of the mitochondrial electron transport chain enzyme, CoQ_{10} (50 μM). At 48 hours after treatment with RSV alone, there was no significant change in basal expression of MnSOD in ARPE-19 cells.

Effect of Resveratrol on Mitochondrial Energy Metabolism

Our observations of a similar reversal by RSV or CoQ_{10} of acrolein-induced increases in MnSOD expression prompted the suggestion of a direct effect of RSV on mitochondrial bioenergetic functions. To characterize the effect of RSV on mitochondrial bioenergetics, we measured the OCR and the ECAR in ARPE-19 cells using Seahorse Bioscience technology. At 24 hours after incubation, high-dose (20 μM) RSV resulted in a significant increase in basal OCR relative to that in the untreated control cells (+21.3 ± 2.1%, $P < 0.05$, $n = 10$) (Figs. 4A, 4B). The complex V inhibitor oligomycin (1 μM) was used to estimate the proportion of the basal OCR coupled to ATP synthesis. Following the addition of oligomycin, the percentage declines in OCR in the RSV-treated cells (10 μM: −56.7 ± 4.6%; 20 μM: −58.3 ± 5.7%, $n = 10$) were comparable to that in control cells (−54.6 ± 5.6%, $n = 10$), indicating that ATP turnover was not significantly affected by RSV treatment (Fig. 4B). The mitochondrial uncoupling agent FCCP (0.25 μM) was subsequently used to further determine maximal respiratory capacity. After the addition of FCCP, OCR showed a substantially greater increase in ARPE-19 cells treated with RSV. The last step of the experiments was application of the complex III inhibitor antimycin (1 μM) to inhibit the electron transport to complex V. This treatment resulted in a profound suppression of the OCR, and the residual oxygen consumption was accounted for by nonmitochondrial oxygen-consuming pathways.[41] The comparable residual OCR values measured in control (35 ± 3.5 pmol/min, $n = 10$) and RSV-treated (10 μM: 32 ± 2.6 pmol/min, $n = 10$; 20 μM: 31 ± 3.2 pmol/min, $n = 10$) ARPE-19 cells following antimycin application further

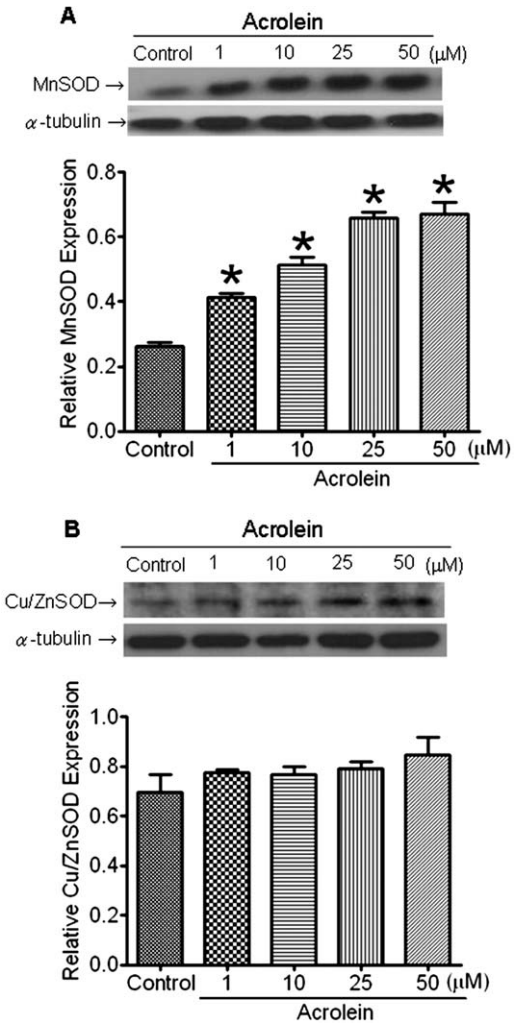

Figure 2. Increases in MnSOD expression following exposure of ARPE cells to acrolein. ARPE-19 cells were treated with acrolein (1, 10, 25, or 50 μM) for 24 hours, and the resultant change in protein expression of manganese superoxide dismutase (MnSOD) (**A**) or copper/zinc SOD (Cu/ZnSOD) (**B**) was assayed by Western blotting. Representative gels (*inset*) and densitometric analysis of protein level of SOD demonstrated that acrolein treatment resulted in a significant increase in MnSOD expression in ARPE cells. Data are mean ± SEM. $^*P < 0.05$ versus untreated control group.

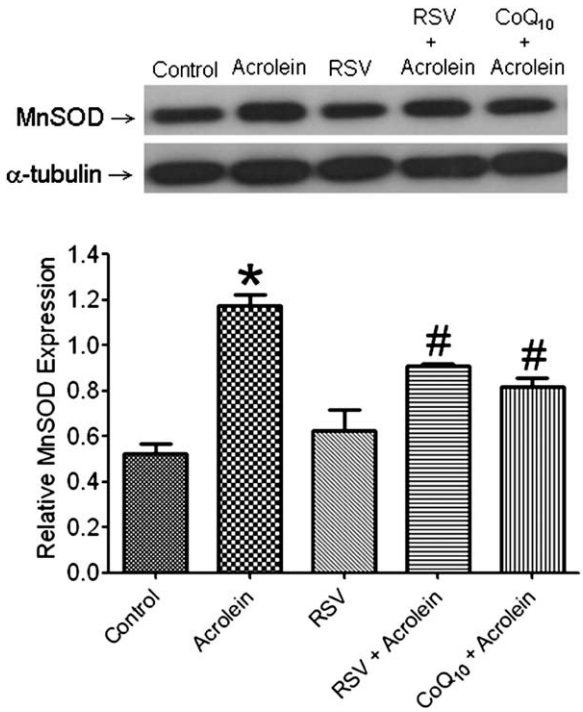

Figure 3. Reversal by resveratrol of acrolein-induced upregulation of MnSOD expression in ARPE cells. ARPE-19 cells were pretreated with resveratrol (RSV; 20 μM) or coenzyme Q_{10} (CoQ_{10}; 50 μM) for 48 hours and then exposed to acrolein (25 μM) for 24 hours. Expression of MnSOD was determined by Western blot analysis. Representative gels (*inset*) and densitometric analysis of protein level of MnSOD demonstrated that acrolein-induced upregulation of MnSOD expression was significantly attenuated by RSV treatment. Data are mean ± SEM. $^*P < 0.05$ versus control group; $^\#P < 0.05$ versus acrolein-treated group.

confirmed the specificity of RSV to increase mitochondrial bioenergetics.

Measurement of ECAR reflects lactate production and is used as an index of glycolytic activity of cells.[40] We found that there was a significantly lower ECAR in the RSV-treated cells (Figs. 4C, 4D), indicating a decrease in glycolysis of the treated cells in a dose-related manner. The increase in ECAR following the addition of oligomycin was used to indicate a shift to ATP production by glycolysis via the Pasteur effect.[48] A lesser increase in ECAR of the RSV-treated (10 μM: +36.8 ± 10.5%; 20 μM: +43.8 ± 7.4%, $n = 10$) versus control (+59.3 ± 8.3%, $n = 10$) cells suggests that the overall energy production in ARPE-19 cells depends more on oxidative phosphorylation than on glycolysis under RSV treatment (Fig. 4D). These findings were further confirmed by analysis of the ratio of OCR to ECAR (Figs. 4E, 4F), which showed that the ratio of oxygen consumption to extracellular acidification, ATP synthesis via oxidative phosphorylation, and maximal respiratory capacity of oxidative phosphorylation were all significantly higher in cells exposed to RSV. Given that high-concentration (20 μM) RSV resulted in a significant increase in mitochondrial energy metabolism, this concentration was used in the subsequent experiments.

Resveratrol Protects Against Acrolein-Induced Inhibition of Mitochondrial Bioenergetics

After 48-hour exposure, acrolein (25 μM) caused a significant reduction in maximal respiratory capacity but no discernible change in basal respiration or ATP turnover in ARPE-19 cells (Figs. 5A, 5B). Resveratrol pretreatment for 24 hours converted the acrolein-induced decrease to an increase in the maximal respiration capacity of the mitochondria. In addition, acrolein exposure had no effect on ECAR values, glycolysis-associated ATP turnover, or respiratory capacity, and these parameters were not affected by RSV pretreatment (Figs. 5C, 5D). Analysis of the ratio of OCR to ECAR demonstrated that oxygen consumption over extracellular acidification rate and maximal respiratory capacity of oxidative phosphorylation was significantly decreased by acrolein (Figs. 5E, 5F). Resveratrol pretreatment converted the ratio of OCR to ECAR to an increase and preserved mitochondrial respiratory capacity of oxidative phosphorylation, indicating that RSV caused preservation of energy production in the acrolein-treated cells mainly from oxidative phosphorylation (Fig. 5F).

Investigative Ophthalmology & Visual Science

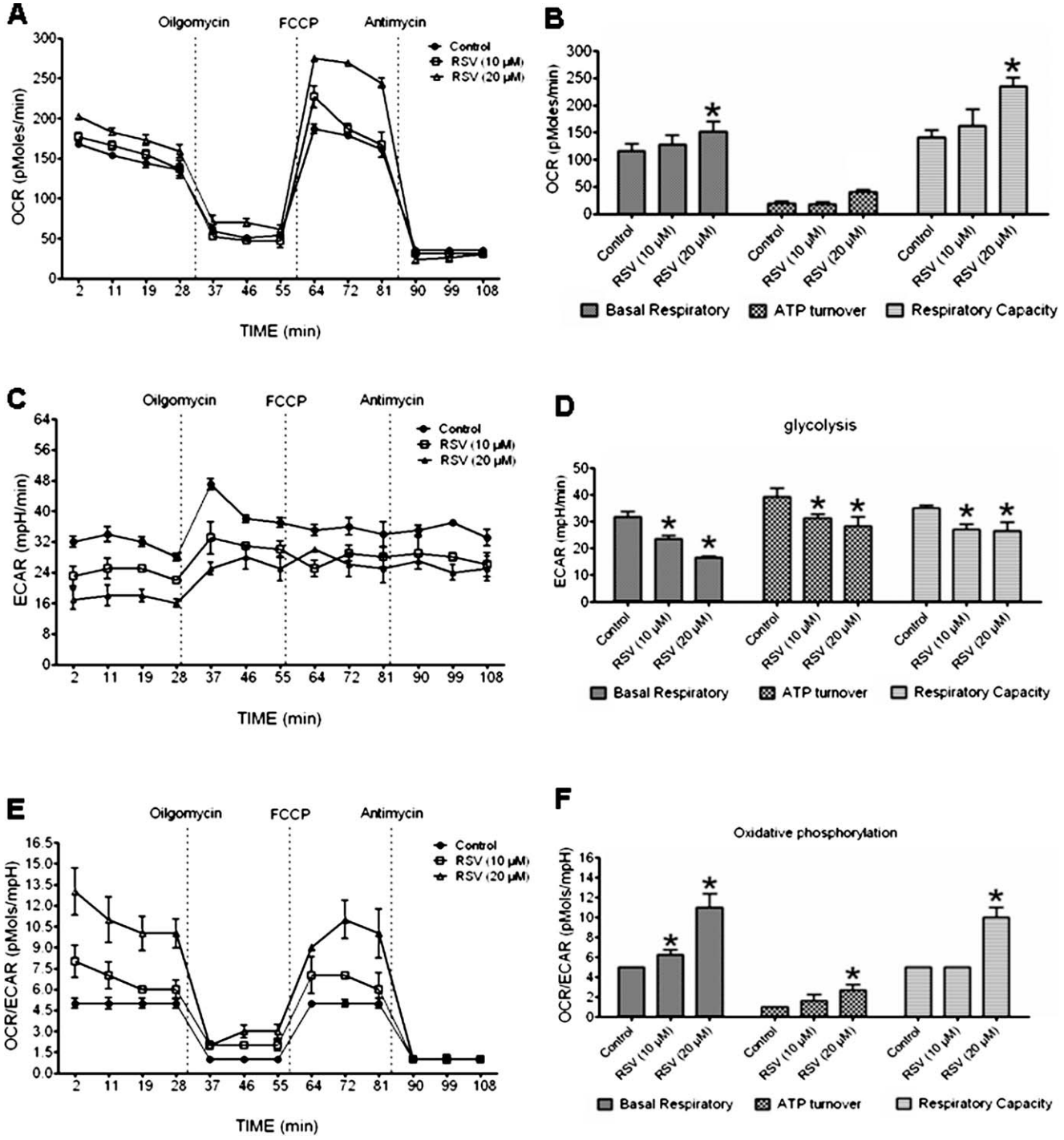

FIGURE 4. Resveratrol increases cellular energy metabolism in ARPE-19 cells. ARPE-19 cells were treated with RSV (10 or 20 μM) for 48 hours. The oxygen consumption rate (OCR) and extracellular acidification rate (ECAR) were determined using Seahorse XF-24 Metabolic Flux Analyzer. (**A**, **C**, **E**) Group data of original tracing showing changes in OCR, ECAR, and the ratio of OCR to ECAR in response to the sequential administration (*vertical lines*) of oligomycin (1 μM), carbonyl cyanide 4-(trifluoromethoxy)phenylhydrazone (FCCP; 0.25 μM), and antimycin (1 μM) to ARPE cells treated with RSV (20 μM) for 24 hours. (**B**, **D**, **F**) Bar graphs of data collected from 10 independent experiments. RSV treatment increased both basal respiration and maximal respiratory capacity of mitochondria in ARPE cells. The same treatment also decreased glycolysis and increased cellular energy production via oxidative phosphorylation. Data are mean ± SEM. $^*P < 0.05$ versus corresponding control group.

Effect of Resveratrol on Mitochondrial Biogenesis

To test whether the observed changes in mitochondrial bioenergetics with various treatments were associated with alterations in mitochondrial biogenesis, the relative mtDNA copy number and expression of mtTFA mRNA (one of the major transcription factors in the regulation of mitochondrial biogenesis[49]) were evaluated. In comparison to the untreated ARPE-19 cells, the relative mitochondrial copy number (Fig. 6A) and expression of mtTFA mRNA (Fig. 6B) were not affected following 24-hour treatment with acrolein (25 μM) alone or with added RSV (20 μM) or CoQ_{10} (50 μM) treatment.

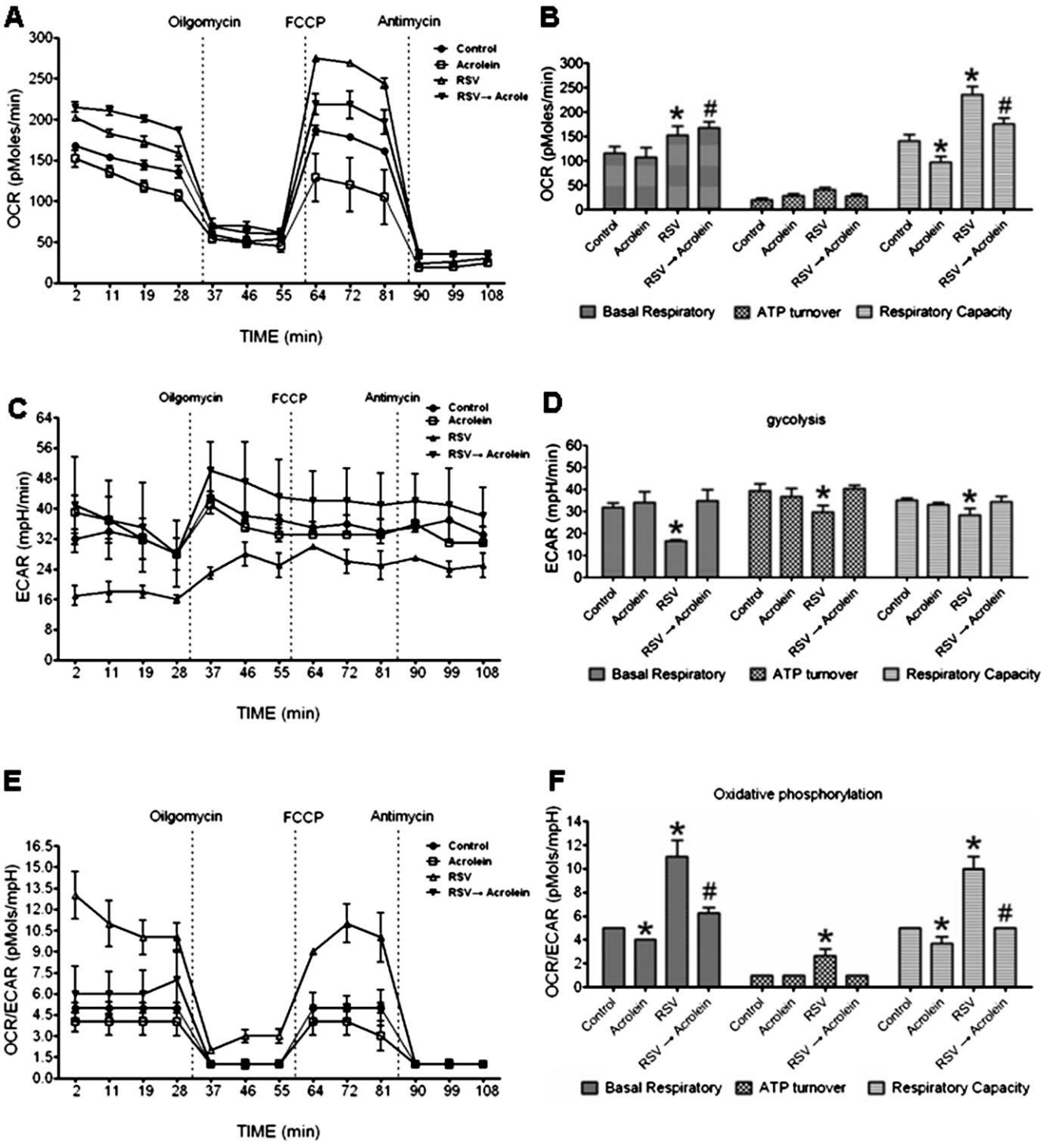

FIGURE 5. Resveratrol protects against acrolein-induced inhibition of mitochondrial bioenergetics of ARPE-19 cells. ARPE-19 cells were pretreated with RSV (20 μM) for 48 hours, followed by exposure to acrolein (25 μM) for 24 hours. The OCR and ECAR were determined using Seahorse XF-24 Metabolic Flux Analyzer. (**A**, **C**, **E**) Group data of original tracing showing changes in OCR, ECAR, and ratio of OCR to ECAR in response to the sequential administration (*vertical lines*) of oligomycin (1 μM), FCCP (0.25 μM), and antimycin (1 μM). (**B**, **D**, **F**) Bar graphs of data collected from 10 independent experiments. Acrolein exposure decreased maximal respiratory capacity of mitochondria and mitochondrial oxidative phosphorylation in ARPE cells. This inhibition of mitochondrial bioenergetics by acrolein was reversed by the pretreatment with RSV. Data are mean ± SEM. $^*P < 0.05$ versus corresponding control group; $\#P < 0.05$ versus acrolein-treated group.

Resveratrol Inhibits Laser-Induced Choroidal Neovascularization in Rodent Eyes

Laser-induced CNV in rodent eyes has been used as a surrogate for the study of abnormal angiogenesis in eyes of AMD patients.[50] In the RPE–choroidal–sclera flat mounts showing FAG of all four lesion sites, we found that in comparison to the retina of control rats (Figs. 7A, 7H) or rats exposed to air (Figs. 7B, 7H), eyes of rats that received a 4-week long-term intermittent CS exposure exhibited a

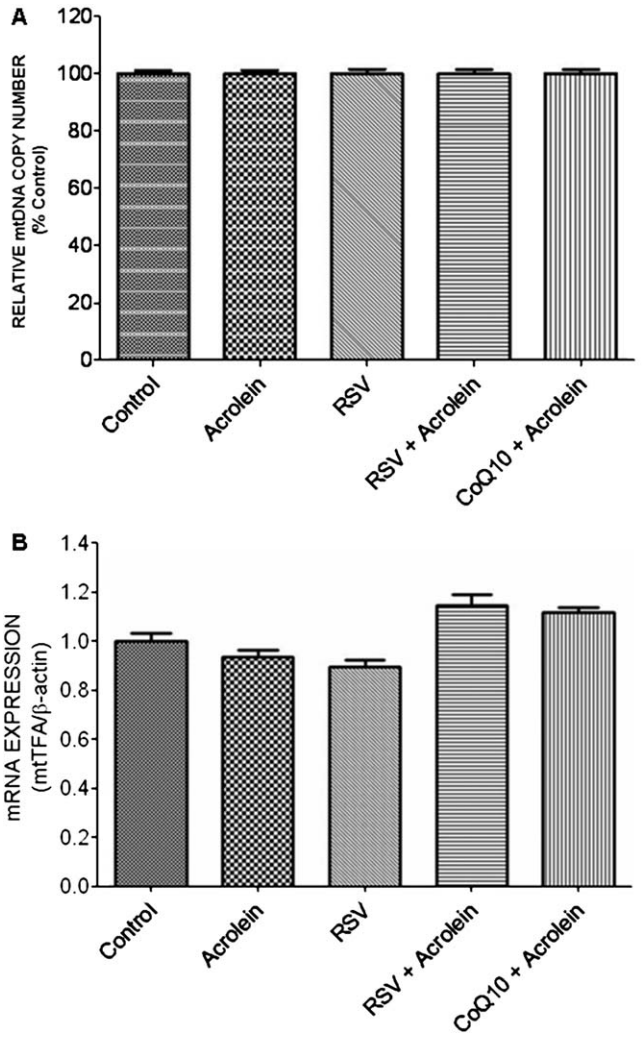

FIGURE 6. Acrolein alone or with additional resveratrol treatment has no effect on mitochondrial biogenesis of ARPE-19 cells. Changes in the relative mitochondrial DNA (mtDNA) copy number (**A**) or mRNA expression of mitochondrial transcription factor A (mtTFA) (**B**) in the ARPE-19 cells treated for 24 hours with acrolein (25 μM) alone or with added resveratrol (RSV, 10 or 20 μM). The mtDNA copy number and mtTFA mRNA expression were determined by quantitative RT-PCR. Each PCR reaction was done in duplicate, and experiments were repeated for three independent cell cultures. The mtDNA copy number was defined as total mtDNA copies divided by total nuclear DNA (nDNA) copies. The mtNDA copy number for control ARPE-19 cells is denoted as 100%. Data are mean ± SEM, $n = 3$. No significant difference among the treated groups in one-way analysis of variance.

significant increase in the area of CNV induced by laser irradiation (Figs. 7E, 7H). This CS-induced increased in CNV following laser injury was appreciably prevented in rats subjected to pretreatment with intraperitoneal infusion of RSV (1.6 mg/kg/d) (Figs. 7F, 7H) or CoQ_{10} (0.36 mg/kg/d) (Figs. 7G, 7H). Under the same treatment regimen and dosing, RSV (Figs. 7C, 7H) and CoQ_{10} (Figs. 7D, 7H) treatment alone exhibited moderate protection against laser-induced CNV in rats exposed to air. In a separate series of experiments, we found that CS exposure did not affect the relative mtDNA copy number in the primary culture of rodent RPE cells (–9.2 ± 4%; $P > 0.05$, $n = 3$), nor did additional RSV treatment (+10.5 ± 5%; $P > 0.05$, $n = 3$).

DISCUSSION

In the present study we provide evidence to suggest that an increase in mitochondrial bioenergetics may account for the cytoprotective effect of RSV against acrolein-induced cell damage and oxidative stress in ARPE-19 cells, as well as the CS-induced exacerbation of laser-induced CNV in rodent eyes. We found that RSV treatment alone significantly increased basal respiratory rate and maximal respiratory capacity in the mitochondria. It also decreased energy dependence on glycolysis and shifted ATP production to oxidative phosphorylation. These functions are related to the protective effect of RSV against an acrolein-induced decrease in cell viability and oxidative stress in a cell model of human AMD, as well as to amelioration of the increase in laser-induced CNV in animals subjected to long-term CS exposure. Resveratrol has been reported to exert cytoprotection in the eyes via its antioxidant activity.[31,32,51] Results of the present study add a novel mechanism of action for the cytoprotective effect in the eyes through this major polyphenol found in red wine.

Accumulating evidence on the susceptibility of mtDNA to oxidative stress damage in ARPE cells, together with the age-related deterioration of the mitochondrial antioxidant defense system, provides the rationale for a mitochondria-based model of human AMD.[15] In contrast to most studies that focus on the antioxidant effects of RSV in protecting ARPE cells from oxidative stress,[11,31,33,52] our results unravel a direct stimulatory effect of RSV on mitochondrial bioenergetics. We further reasoned that this beneficial effect of RSV on mitochondrial bioenergetics is achieved by at least two mechanisms. One is through the increase in maximal capacity of oxidative phosphorylation, and the second is through the shift of energy production from a less effective anaerobic glycolysis to a highly efficient aerobic oxidative phosphorylation. The stimulatory action of RSV in bioenergetics does not result from the increase in mitochondrial biogenesis. We found that RSV has no effect on the relative mtDNA copy number or expression of mtTFA, a transcription factor essential for regulation of replication and transcription of mtDNA.[49] Human RPE cells are enriched with mitochondria for a robust metabolic activity to meet the high-energy demands of the cells. Mitochondrial dysfunction contributes to generation of ROS in the RPE cells.[14] RSV may thus protect ARPE cells from oxidative stress through its action to directly increase the mitochondrial bioenergetics.

Acrolein is a common environmental, food, and water pollutant and a major toxic ingredient of CS. In addition, acrolein can be produced endogenously via lipid peroxidation and by normal cellular metabolism.[53] Acrolein is known to possess diverse toxic effects in various cell types. In human RPE cells, we found that exposure to acrolein at 25 μM over 24 to 72 hours caused significant loss of cell viability and suppression of mitochondrial bioenergetics. These results are in parallel to the reported cytotoxicity of acrolein.[18,34] Mechanisms underlying acrolein-induced cell death in the ARPE-19 cells are not immediately clear in this study. In this regard, both apoptosis and necrosis have been reported.[54,55] Decrease in mitochondrial oxygen consumption in the outer retina is also involved in gradual cone cell death from oxidative damage.[15,16] Acrolein decreases the enzyme activity of mitochondrial electron transport complexes I, II, and III, resulting in an increase in superoxide levels in the organelle.[27] Together with our observations of a reduction in the maximal respiratory capacity and oxidative phosphorylation of mitochondria, these results strongly suggest acrolein as a potent mitochondrial toxicant in RPE cells. Acrolein was reported to exert its cytotoxicity via decreasing expression and activity of antioxidants.[27,47] Intriguingly, we found in the present study

Investigative Ophthalmology & Visual Science

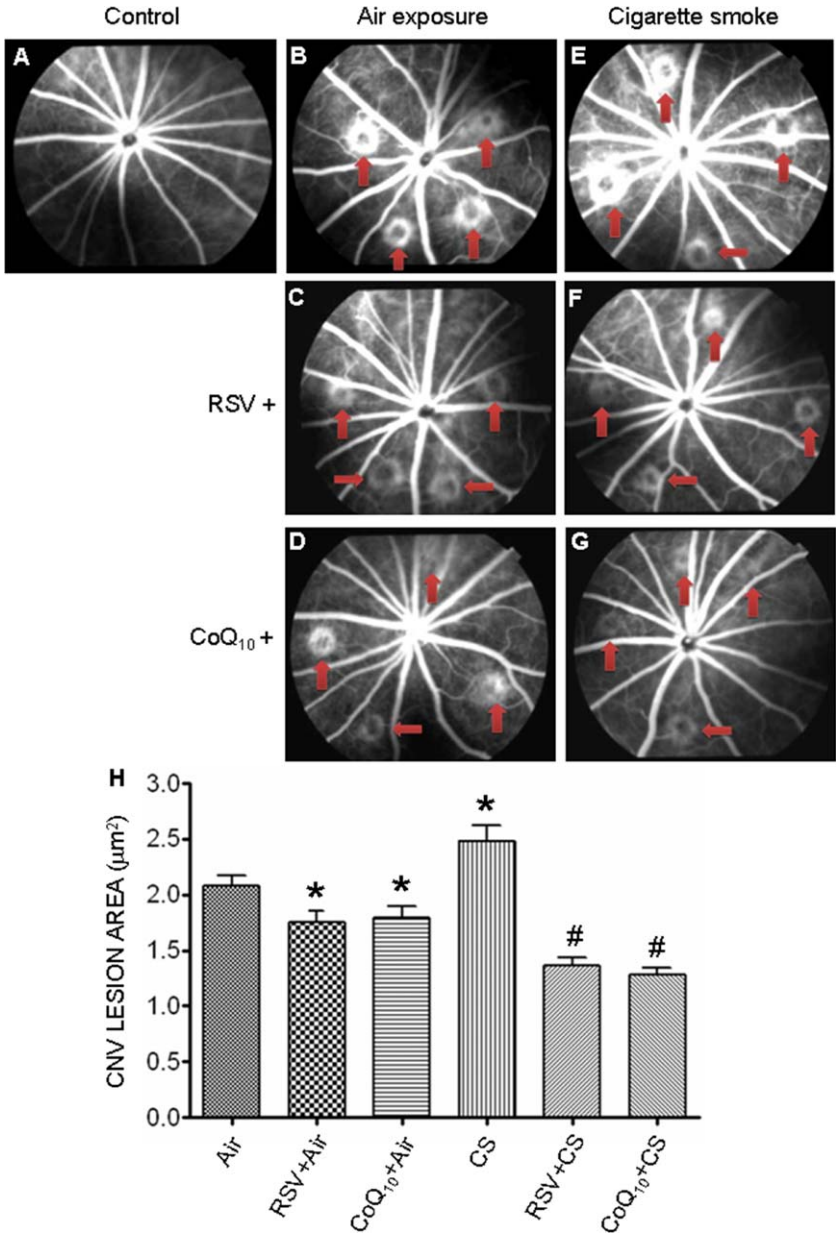

Figure 7. Resveratrol protects against laser-induced choroidal neovascularization. Representative original photomicrographs (**A–G**, *top*) and bar graphs (*bottom*) show all four lesion sites of laser-induced photocoagulation in rodent eyes under various conditions. The areas of CNV lesions were determined by fundus fluorescein angiography (FAG). Animals were exposed to cigarette smoke (CS) in an exposure chamber. RSV (1.6 mg/kg/d), CoQ_{10} (0.36 mg/kg/d), or vehicle (0.8% DMSO) was infused into the peritoneal cavity of animals via an osmotic minipump. Laser irradiation-induced CNV was exacerbated by CS exposure. Both RSV and CoQ_{10} infusion blocked the increase in laser-induced CNV in animals exposed to CS. Data are mean ± SEM, $n = 5$ in each group. $^{*}P < 0.01$ versus vehicle group; $\#P < 0.01$ versus vehicle + CS group.

that acrolein caused an increase, instead of a decrease, in mitochondrial MnSOD expression in ARPE-19 cells. This finding was interpreted as arguing for the activation of a cellular compensatory mechanism to counterbalance the oxidative stress induced by acrolein. Our results of an increase in MnSOD but not Cu/ZnSOD or ecSOD expression by acrolein further point to the importance of mitochondrial oxidative stress in mediating cytotoxicity of acrolein in RPE cells.

A direct action of RSV on mitochondrial bioenergetics contributes to the protection against acrolein-induced cytotoxicity in ARPE-19 cells. Pretreatment with RSV reversed inhibition by acrolein of the mitochondrial bioenergetics and shifted cellular energy dependence from glycolysis to oxidative phosphorylation. These functions are related to its protective effects against acrolein-induced decrease in cell viability and oxidative stress. Coenzyme Q_{10}, a mobile mitochondrial electron carrier, was reported to alleviate mitochondrial oxidative stress by increasing mitochondrial bioenergetics.[56] This compound was used in the present study as a positive control to confirm the mitochondrial protective effect of RSV. We noted that the dose of RSV (10 or 20 μM) used in the present study was less than those (25–100 μM) reported to directly scavenge ROS.[57] It is thus deemed unlikely that protection against acrolein-induced cell damage is attributable to a direct antioxidant effect of RSV. This notion is further

supported by the findings of a negligible effect of RSV on expression of SOD isoforms in ARPE cells.

Laser-induced CNV in rodent eyes has been used as a surrogate for the study of abnormal angiogenesis in eyes of AMD patients.[50] Oxidative stress is known to play an active role in the development of CNV. Application of a pro-oxidant stressor increases amounts of vascular endothelial growth factor in choroidal endothelial cells and promotes CNV.[58] Treating mice with antioxidants, on the other hand, suppresses the development of CNV.[58,59] Moreover, older *Sod1*$^{-/-}$ knockout mice display a thickened Bruch's membrane and develop CNV.[60] In this study, we found that long-term intermittent exposure to CS for 4 weeks significantly increased, and RSV pretreatment appreciably reversed, laser-induced CNV in rat eyes. Acrolein, which was demonstrated in our in vitro study to be a potent mitochondrial oxidant, is a major toxicant constituent of CS. In our in vitro study we found that RSV antagonized acrolein-induced oxidative stress and loss of cell viability via its action to increase mitochondrial bioenergetics; it is thus conceivable that the same mechanism may contribute to the protection against CS-promoted increase in CNV in rat eyes. Our data from primary culture of rat RPE cells indicate that CS alone or with RSV pretreatment has no detectable effect on the relative mtDNA copy number. We recognize that the use of FAG may not be the most appropriate method for measuring laser-induced CNV, as the fluorescence may leak out from the choroidal blood vessels during tissue preparation. In this regard, the use of an antibody with high binding affinity to endothelial cells, such as anti-intercellular adhesion molecule-1, may provide better quantification.

Resveratrol or CoQ_{10} alone exerts moderate protection against laser-induced development of CNV. This protection becomes prominent in animals subjected to long-term CS. The in vivo study involved a much more complicated pathway than the in vitro study, and animals possess natural antioxidants to protect against the oxidative stress in routine life. This might explain why RSV or CoQ_{10} alone exerted only modest protection against laser-induced CNV injury. Once oxidative stress is induced by CS, natural antioxidants might not be sufficient to maintain redox homeostasis, and additional nutritional supplements are hence required to protect the eyes against the oxidative stress. In support of this suggestion, in a large-scale randomized controlled clinical trial on age-related eye disease, a 5-year follow-up survey showed that nutritional supplementation had a 25% beneficial effect in reducing the risk of advanced AMD in patients with intermediate AMD.[61]

In conclusion, our results showed that acrolein caused oxidative damage by inhibiting energy metabolism in the mitochondria of ARPE-19 cells. Resveratrol protected the RPE cells against oxidative damage through a direct stimulatory action on mitochondrial bioenergetics. The same mechanism is associated with the protection by RSV against CS-promoted development of CNV. Together these results suggest that RSV might be useful as an adjunctive nutrient supplement in high-risk AMD candidates.

Acknowledgments

Supported by Grants NSC100-2314-B-075B-002 and NSC101-2314-B-075B-006 (S-JS) from the National Science Council, Taiwan; Grants VGHKS 100-065, 101-025, and 102-028 (S-JS) from Kaohsiung Veterans General Hospital; and Grants OMRPG8C0031 and CMRPG8C0051 (JYHC) from the Chang Gung Medical Foundation, Taiwan, Republic of China.

Disclosure: **S.-J. Sheu**, None; **N.-C. Liu**, None; **C.-C. Ou**, None; **Y.-S. Bee**, None; **S.-C. Chen**, None; **H.-C. Lin**, None; **J.Y.H. Chan**, None

References

1. Green WR, McDonnell PJ, Yeo JH. Pathologic features of senile macular degeneration. *Ophthalmology*. 1985;92:615–627.
2. Spraul CW, Lang GE, Grossniklaus HE. Morphometric analysis of the choroid, Bruch's membrane, and retinal pigment epithelium in eyes with age-related macular degeneration. *Invest Ophthalmol Vis Sci*. 1996;37:2724–2735.
3. Cai J, Wu M, Nelson KC, Sternberg P Jr, Jones DP. Oxidative damage and protection of the RPE. *Prog Retin Eye Res*. 2000; 19:205–221.
4. Liang FQ, Godley BF. Oxidative stress-induced mitochondrial DNA damage in human retinal pigment epithelial cells: a possible mechanism for RPE aging and age-related macular degeneration. *Exp Eye Res*. 2003;76:397–403.
5. Winkler BS, Boulton ME, Gottsch JD, Sternberg P. Oxidative damage and age-related macular degeneration. *Mol Vis*. 1999; 5:32–33.
6. Shen JK, Dong A, Hackett SF, Bell WR, Green WR, Campochiaro PA. Oxidative damage in age-related macular degeneration. *Histol Histopathol*. 2007;22:1301–1308.
7. Ballinger SW, Van Houten B, Conklin CA, Jin GF, Godley BF. Hydrogen peroxide causes significant mitochondrial DNA damage in human RPE cells. *Exp Eye Res*. 1999;68:765–772.
8. Cai J, Wu M, Nelson KC, Sternberg P Jr, Jones DP. Oxidant induced apoptosis in cultured human retinal pigment epithelial cells. *Invest Ophthalmol Vis Sci*. 1999;40:959–966.
9. Garg TK, Chang JY. Oxidative stress causes ERK phosphorylation and cell death in cultured retinal pigment epithelium: prevention of cell death by AG126 and 15-deoxy-delta 12, 14-PGJ2. *BMC Ophthalmol*. 2003;21:3–5.
10. Jin GF, Hurst JS, Godley BF. Hydrogen peroxide stimulates apoptosis in cultured human retinal pigment epithelial cells. *Curr Eye Res*. 2001;22:165–173.
11. Evans J. Antioxidant supplements to prevent or slow down the progression of AMD: a systematic review and meta-analysis. *Eye*. 2008;22:751–760.
12. Evans JR, Lawrenson JG. Antioxidant vitamin and mineral supplements for preventing age-related macular degeneration. *Cochrane Database Syst Rev*. 2012;13:CD000253.
13. Zeng R, Zhang Y, Shi F, Kong F. A novel experimental mouse model of retinal detachment: complete functional and histologic recovery of the retina. *Invest Ophthalmol Vis Sci*. 2012;53:1685–1695.
14. Lianga FO, Godley BF. Oxidative stress-induced mitochondrial DNA damage in human retinal pigment epithelial cells: a possible mechanism for RPE aging and age-related macular degeneration. *Exp Eye Res*. 2003;76:397–403.
15. Barot M, Gokulgandhi MR, Mitra AK. Mitochondrial dysfunction in retinal diseases. *Curr Eye Res*. 2011;36:1069–1077.
16. Van Bergen NJ, Chakrabarti R, O'Neill EC, Crowston JG, Trounce IA. Mitochondrial disorders and the eye. *Eye Brain*. 2011;3:29–47.
17. Plafker SM, O'Mealey GB, Szweda LI. Mechanisms for countering oxidative stress and damage in retinal pigment epithelium. *Int Rev Cell Mol Biol*. 2012;298:135–165.
18. Thornton J, Edwards R, Mitchell P, Harrison RA, Buchan I, Kelly SP. Smoking and age-related macular degeneration: a review of association. *Eye*. 2005;19:935–944.
19. Khan JC, Thurlby DA, Shahid H, et al. Smoking and age related macular degeneration: the number of pack years of cigarette smoking is a major determinant of risk for both geographic atrophy and choroidal neovascularisation. *Br J Ophthalmol*. 2006;90:75–80.
20. Tomany SC, Wang JJ, Van Leeuwen R, et al. Risk factors for incident age-related macular degeneration: pooled findings from 3 continents. *Ophthalmology*. 2004;111:1280–1287.

21. Evans JR, Fletcher AE, Wormald RP. 28,000 Cases of age related macular degeneration causing visual loss in people aged 75 years and above in the United Kingdom may be attributable to smoking. *Br J Ophthalmol*. 2005;89:550–553.
22. Clemons TE, Milton RC, Klein R, Seddon JM, Ferris FL III; AREDS Research Group. Risk factors for the incidence of advanced age-related macular degeneration in the Age-Related Eye Disease Study (AREDS). AREDS report no. 19. *Ophthalmology*. 2005;112:533–539.
23. Lykkesfeldt J, Christen S, Wallock LM, Chang HH, Jacob RA, Ames BN. Ascorbate is depleted by smoking and repleted by moderate supplementation: a study in male smokers and nonsmokers with matched dietary antioxidant intakes. *Am J Clin Nutr*. 2000;71:530–536.
24. O'Neill CA, Halliwell B, van der Vliet A, et al. Aldehyde-induced protein modifications in human plasma: protection by glutathione and dihydrolipoic acid. *J Lab Clin Med*. 1994;124:359–370.
25. Cross CE, O'Neill CA, Reznick AZ, et al. Cigarette smoke oxidation of human plasma constituents. *Ann N Y Acad Sci*. 1993;686:72–89.
26. Fowles J, Dybing E. Application of toxicological risk assessment principles to the chemical constituents of cigarette smoke. *Tob Control*. 2003;12:424–430.
27. Jia L, Liu Z, Sun L, et al. Acrolein, a toxicant in cigarette smoke, causes oxidative damage and mitochondrial dysfunction in RPE cells: protection by (R)-α-lipoic acid. *Invest Ophthalmol Vis Sci*. 2007;48:339–348.
28. Lin H, Xu H, Liang FQ, et al. Mitochondrial DNA damage and repair in RPE associated with aging and age-related macular degeneration. *Invest Ophthalmol Vis Sci*. 2011;52:3521–3529.
29. Pervaiz S. Resveratrol: from grapevines to mammalian biology. *FASEB J*. 2003;17:1975–1985.
30. Jang JH, Surh YJ. Protective effects of resveratrol on hydrogen peroxide-induced apoptosis in rat pheochromocytoma (PC12) cells. *Mutat Res*. 2001;496:181–190.
31. Kubota S, Kurihara T, Mochimaru H, et al. Prevention of ocular inflammation in endotoxin-induced uveitis with resveratrol by inhibiting oxidative damage and nuclear factor-κ. *Invest Ophthalmol Vis Sci*. 2009;50:3512–3519.
32. Li C, Wang L, Huang K, Zheng L. Endoplasmic reticulum stress in retinal vascular degeneration: protective role of resveratrol. *Invest Ophthalmol Vis Sci*. 2012;53:3241–3249.
33. Luna C, Li G, Liton PB, et al. Resveratrol prevents the expression of glaucoma markers induced by chronic oxidative stress in trabecular meshwork cells. *Food Chem Toxicol*. 2009;47:198–204.
34. Sheu SJ, Liu NC, Chen JL. Resveratrol protects human retinal pigment epithelial cells from acrolein-induced damage. *J Ocul Pharmacol Ther*. 2010;26:231–236.
35. Sheu SJ, Wu TT. Resveratrol protects against ultraviolet A-mediated inhibition of the phagocytic function of human retinal pigment epithelial cells via large-conductance calcium-activated potassium channels. *Kaohsiung J Med Sci*. 2009;25:381–388.
36. Young TA, Wang H, Munk S, et al. Vascular endothelial growth factor expression and secretion by retinal pigment epithelial cells in high glucose and hypoxia is protein kinase C-dependent. *Exp Eye Res*. 2005;80:651–662.
37. Cho KS, Yoon YH, Choi JA, Lee SJ, Koh JY. Induction of autophagy and cell death by tamoxifen in cultured retinal pigment epithelial and photoreceptor cells. *Invest Ophthalmol Vis Sci*. 2012;53:5344–5353.
38. Grigsby J, Betts B, Vidro-Kotchan E, Culbert R, Tsin A. A possible role of acrolein in diabetic retinopathy: involvement of a VEGF/TGF-β signaling pathway of the retinal pigment epithelium in hyperglycemia. *Curr Eye Res*. 2012;37:1045–1053.
39. Nakajima Y, Inokuchi Y, Nishi M, Shimazawa M, Otsubo K, Hara H. Coenzyme Q10 protects retinal cells against oxidative stress in vitro and in vivo. *Brain Res*. 2008;1226:226–233.
40. Modis K, Gero D, Erdelyi K, Szoleczky P, DeWitt D, Szabo C. Cellular bioenergetics is regulated by PARP1 under resting conditions and during oxidative stress. *Biochem Pharmacol*. 2012;83:633–643.
41. Dranka BP, Hill BG, Darley-Usmar VM. Mitochondrial reserve capacity in endothelial cells: the impact of nitric oxide and reactive oxygen species. *Free Radic Biol Med*. 2010;48:905–914.
42. Lin CS, Lee HT, Lee SY, et al. High mitochondrial DNA copy number and bioenergetic function are associated with tumor invasion of esophageal squamous cell carcinoma cell lines. *Int J Mol Sci*. 2012;13:11228–11246.
43. Tang GJ, Wang HT, Wang JY, et al. Novel role of AMP-activated protein kinase signaling in cigarette smoke induction of IL-8 in human lung epithelial cells and lung inflammation in mice. *Free Radic Biol Med*. 2011;50:1492–1502.
44. Sheu SJ, Chou LC, Bee YS, et al. Suppression of choroidal neovascularization by intramuscular polymer-based gene delivery of vasostatin. *Exp Eye Res*. 2005;81:673–679.
45. Khan AA, Dace DS, Ryazanov AG, Kelly J, Apte RS. Resveratrol regulates pathologic angiogenesis by a eukaryotic elongation factor-2 kinase-regulated pathway. *Am J Pathol*. 2010;177:481–492.
46. Hua J, Guerin KI, Chen J, et al. Resveratrol inhibits pathologic retinal neovascularization in Vldlr(-/-) mice. *Invest Ophthalmol Vis Sci*. 2011;52:2809–2816.
47. Feng Z, Liu Z, Li X, et al. α-Tocopherol is an effective phase II enzyme inducer: protective effects on acrolein-induced oxidative stress and mitochondrial dysfunction in human retinal pigment epithelial cells. *J Nutr Biochem*. 2010;21:1222–1231.
48. Guppy M, Abas L, Arthur PG, Whisson ME. The Pasteur effect in human platelets: implications for storage and metabolic control. *Br J Haematol*. 1995;91:752–757.
49. Ekstrand MI, Falkenberg M, Rantanen A, et al. Mitochondrial transcription factor A regulates mtDNA copy number in mammals. *Hum Mol Genet*. 2004;13:935–944.
50. Grossniklaus HE, Kang SJ, Berglin L. Animal models of choroidal and retinal neovascularization. *Prog Retin Eye Res*. 2010;29:500–519.
51. Pintea A, Rugină D, Pop R, Bunea A, Socaciu C, Diehl HA. Antioxidant effect of trans-resveratrol in cultured human retinal pigment epithelial cells. *J Ocul Pharmacol Ther*. 2011;27:315–321.
52. King RE, Kent KD, Bomser JA. Resveratrol reduces oxidation and proliferation of human retinal pigment epithelial cells via extracellular signal-regulated kinase inhibition. *Chem Biol Interact*. 2005;151:143–149.
53. Stevens JF, Maier CS. Acrolein: sources, metabolism, and biomolecular interactions relevant to human health and disease. *Mol Nutr Food Res*. 2008;52:7–25.
54. Kern JC, Kehrer JP. Acrolein-induced cell death: a caspase-influenced decision between apoptosis and oncosis/necrosis. *Chem Biol Interact*. 2002;139:79–95.
55. Mansoor S, Gupta N, Patil AJ, et al. Inhibition of apoptosis in human retinal pigment epithelial cells treated with benzo(e)-pyrene, a toxic component of cigarette smoke. *Invest Ophthalmol Vis Sci*. 2010;51:2601–2607.
56. Bergamini C, Moruzzi N, Sblendido A, Lenaz G, Fato R. A water soluble CoQ10 formulation improves intracellular distribution and promotes mitochondrial respiration in cultured cells. *PLoS One*. 2012;7:e33712.

Investigative Ophthalmology & Visual Science

57. Pintea A, Rugină D, Pop R, Bunea A, Socaciu C, Diehl HA. Antioxidant effect of trans-resveratrol in cultured human retinal pigment epithelial cells. *J Ocul Pharmacol Ther*. 2011;27:315–321.
58. Eichler W, Reiche A, Yafai Y, Lange J, Wiedemann P. Growth-related effects of oxidant-induced stress on cultured RPE and choroidal endothelial cells. *Exp Eye Res*. 2008;87:342–348.
59. Hara R, Inomata Y, Kawaji T, et al. Suppression of choroidal neovascularization by N-acetyl-cysteine in mice. *Curr Eye Res*. 2010;35:1012–1020.
60. Imamura Y, Noda S, Hashizume K, et al. Drusen, choroidal neovascularization, and retinal pigment epithelium dysfunction in SOD1-deficient mice: a model of age-related macular degeneration. *Proc Natl Acad Sci U S A*. 2006;103:11282–11287.
61. Krishnadev N, Meleth AD, Chew EY. Nutritional supplements for age-related macular degeneration. *Curr Opin Ophthalmol*. 2010;21:184–189.

Investigative Ophthalmology & Visual Science